ICARUS **133,** 89–97 (1998)
ARTICLE NO. IS985907

The Opposition Effect of the Moon: Coherent Backscatter *and* Shadow Hiding

Bruce Hapke

Department of Geology and Planetary Science, University of Pittsburgh, Pittsburgh, Pennsylvania 15260
E-mail: hapke@vms.cis.pitt.edu

and

Robert Nelson and William Smythe

Jet Propulsion Laboratory, Pasadena, California 91109

Received July 23, 1997; revised January 22, 1998

The electromagnetic scattering properties of Solar System regoliths are commonly interpreted using the lunar regolith as a prototype. Hence, a thorough understanding of the reflectance of lunar soil is essential to remote sensing planetary studies. We have measured the linearly and circularly polarized reflectances of samples of lunar soil in order to better understand the nature of the lunar opposition effect. Several independent observations show that the zero-phase peak is caused by both shadow hiding and coherent backscatter in roughly equal amounts. Any radiative transfer model for planetary regoliths must take this dual nature into account. The transport mean free path for photons in the lunar regolith is about 1 μm, which is much smaller than the mean particle size.

INTRODUCTION

The opposition effect is the narrow peak in the intensity of light scattered from a particulate medium directly back in the direction toward the source. It is a nearly ubiquitous phenomenon which is exhibited by media as diverse as soils, frosts, and vegetation canopies (Hapke *et al.* 1996). It has been known for over a century, having first been observed in the light received from the rings of Saturn by Seeliger (1895), and was first observed for the moon by Gehrels *et al.* (1964). The brightness of any area on the lunar surface increases by nearly 40% between about one day before full moon and the time of full moon.

During most of the time since its discovery the opposition effect has been interpreted as being caused by shadow hiding, in which particles of a medium cast shadows that are partly visible at all times except near astronomical opposition, when each particle hides its own shadow. (See Hapke, 1986 for a recent treatment of the shadow hiding opposition effect.) However, another process, coherent backscatter, that causes an opposition effect has recently gained widespread attention in several scientific fields (Watson 1969; Kravtsov and Saichev 1982; Kuga and Ishimaru 1984; Van Albada and Lagendijk 1985). In this phenomenon portions of waves traveling in opposite directions along multiply scattered paths within a nonuniform medium interfere constructively with each other to cause a peak at zero phase. It has been suggested by several persons (including Kuga and Ishimaru 1984; Shkuratov 1988; Muinonen 1990; Hapke 1990; Mishchenko and Dlugach 1992) that this phenomenon may contribute to the opposition effect of solar system bodies. Hapke *et al.* (1993) measured the reflectances of Apollo lunar soil samples in circularly polarized light and showed that coherent backscatter is a major contributor to the lunar opposition effect.

The opposition effect is an important tool in remote sensing and contains information about such quantities as porosity and transport mean free path for photons in the soil. Every solar system object whose surface can be seen and whose photometric function has been measured at small phase angles exhibits the phenomenon. However, the moon is the only body (besides the earth) for which we possess samples of regolith, and properties of the regoliths of other objects are commonly interpreted in terms of a lunar model. Both shadow hiding and coherent backscatter are viable mechanisms for producing an opposition effect. Hence, it is important both for the interpretation of planetary remote sensing measurements and for the construction of improved models of light scattering by planetary regoliths to understand whether or not both processes are operating and the role of each.

Recently, Buratti *et al.* (1996) and Helfenstein *et al.* (1997) analyzed Clementine and telescopic lunar data. Bur-

0019-1035/98 $25.00

TABLE I
Opposition Peak Angular Widths

Sample number	Normal albedo[a]	Reverse-helicity HWHM (°)	Same-helicity HWHM (°)
10084	0.078	4.3	1.4
15041	0.094	8.3	2.7
15271	0.128	5.2	1.7
15601	0.102	8.9	1.5
61221	0.375	12.1	3.0
65701	0.153	7.4	2.3
75121	0.083	4.1	1.5
79221	0.084	14.4	3.6
Averages		8.1	2.2

[a] In red light (633 nm).

atti *et al.* concluded that shadow hiding was the dominant mechanism; however, the data cited to support this conclusion can be interpreted in other ways. In particular, the photometric differences between the highland and maria support coherent backscatter. Helfenstein *et al.* concluded that both processes contribute to the opposition effect of the moon. However, this conclusion does not have as strong an observational basis as one would like because it rests rather critically on one data point. In this paper we report further results of laboratory measurements on lunar samples that greatly strengthen and illuminate the conclusion of Helfenstein *et al.*

DESCRIPTION OF SAMPLES AND INSTRUMENTS

The same eight lunar soil samples described in our previous paper (Hapke *et al.* 1993) were used in this study (Table I). They include mature and immature soils from the maria and highlands. The samples were prepared for measurement by gently pouring them from a height of about one cm into a circular cup about 2.5 cm in diameter by 0.5 cm deep. If necessary, a sample was gently shaken to even out its thickness but, in order to mimic its natural condition on the lunar surface as closely as practical, its surface was not pressed or scraped in any way.

The samples were studied using two instruments, a short arm and a long arm goniometric photopolarimeter, both housed in the Goniometric Laboratory at the Jet Propulsion Laboratory. The light source on the short arm instrument was either a Cd laser at 442 nm (blue) or a He–Ne laser at 633 nm (red); only the He–Ne laser was used on the long arm instrument. The detector was a solid state photodiode with sensitive surface about 1 mm in diameter. On the short arm instrument the source and detector were 33 cm from the sample, so that the detector subtended an angle of 0.17° from the sample. On the long arm instrument the corresponding length was 228 cm and the angle 0.025°. The sample was illuminated vertically, and the detector could be moved to view the sample from zenith angles of 1° to 65° for the short arm instrument and from 0.2° to 5° for the long arm. In this configuration, the phase angle g is equal to the viewing angle e. Background noise was minimized by placing a narrow band transmission filter in front of the detector and also by chopping the incident beam and measuring the signal with a synchronous detector.

Linear polarizers and quarter wave plates could be placed between the source and sample and between the sample and detector, allowing the sample to be illuminated and viewed with orthogonal senses of both linearly and circularly polarized light. The observing procedure used was to fix the detector position and measure the intensity in all eight configurations of polarizers and quarter wave plates before moving on to the next detector angle.

A fixed area about 3 mm in diameter was illuminated on the sample surface, while the detector viewed a much larger area. The surface was horizontal, while the scattering plane was tilted by a fraction of a degree from the vertical to insure that no specularly reflected light reached the detector. When a stationary sample was illuminated the usual laser speckle pattern due to constructive and destructive interference of light scattered along different paths within the material was observed (Kaveh *et al.* 1986). Hence, the sample was continuously rotated about its central vertical axis in order to average out this speckle pattern. The main source of noise in the instrument is random laser drift of about ±2% on a time scale of minutes.

THEORETICAL REMARKS

As an aid to understanding the results of the tests carried out on the lunar samples, the processes that occur in light scattering by a particulate medium will be reviewed. The reflectance is made up of the sum of light that has been scattered only once by a particle and light scattered between two or more particles. In a low albedo material the reflectance is dominated by single scattering, while multiple scattering becomes progressively more important as the albedo increases. The shadow hiding opposition effect (SHOE) is caused almost entirely by radiation scattered once, multiply scattered light serving only to fill in the particle shadows. However, the coherent backscatter opposition effect (CBOE) is due to the multiply scattered component.

The opposition effect is concerned with light scattered backwards in the general direction of the source. If the particles of the medium are comparable or smaller than the wavelength, they scatter approximately like polarizable dipoles. If linearly polarized light is incident on a medium of such particles, a single backscattering event tends to

preserve the direction of polarization, but multiple scatterings randomize, or depolarize, this direction. If the incident light is circularly polarized, the handedness, or helicity, of the incident light is reversed upon being backscattered once, but is preserved if the light is scattered into the forward hemisphere.

If the particles of the medium are larger than the wavelength a single backscattering occurs either by specular reflection from the first surface of the particle, or by specular internal reflection from the far surface, or by scattering from internal imperfections. All three processes tend to preserve the direction of incident linear polarization, but reverse the helicity of incident circular polarization. Light is forward scattered by either refraction and transmission through the particle or by diffraction around it, both of which tend to preserve the direction of incident linear polarization and the helicity of incident circular polarization. Multiple scatterings tend to randomize the senses of linear and circular polarization. However, the randomization takes place by rotation of the electric vector, to which the linearly polarized light is much more sensitive than the circularly polarized. Hence, the randomization takes many more scatterings for circularly polarized light than for linearly polarized.

Thus, if a sample is illuminated and observed in linearly polarized light with the source and detector polarizers parallel to each other, the scattered light contains both singly and multiply scattered light that exhibits a strong opposition effect. This peak is caused by both CBOE and SHOE. However, if the transmission axes of the two polarizers are perpendicular, the reflectance consists almost entirely of multiply scattered light whose electric vectors have been randomized in direction. The randomized waves have lost most of their coherence, so that the light has only a weak opposition effect that is mainly CBOE.

By contrast, if the reflectance of a low albedo sample is measured in circularly polarized light in a configuration that measures the opposite sense of helicity as the incident irradiance, the reflectance at small phase angles consists almost entirely of singly scattered light. Thus, any opposition effect observed is mainly SHOE. If the same sense of helicity as incident is detected, the reflectance at small phase angles is made up mostly of light that has been reflected, transmitted or diffracted by two or more particles in such a way as to largely preserve both the helicity and coherence. Hence, the resulting opposition effect is mainly CBOE.

The angular width of a SHOE peak is independent of wavelength, but that of a CBOE proportional to wavelength, the half width at half maximum (HWHM) being given by (Van Albada *et al.* 1990)

$$\mathrm{HWHM} = b\lambda/2\pi L, \quad (1)$$

where λ is the wavelength, b is a constant whose empirical value is 0.36, and L is the transport mean free path for photons in the medium. The usual equation for L in the radiative transfer literature is

$$L = [n\sigma Q_s(1 - \langle\cos\theta\rangle)]^{-1} = [n\sigma w Q_E(1 - \langle\cos\theta\rangle)]^{-1}, \quad (2)$$

where n is the number of particles per unit volume, σ is the mean particle geometrical cross section, Q_s is the mean scattering efficiency, Q_E is the mean extinction efficiency, $w = Q_s/Q_E$ is the mean single scattering albedo and $\langle\cos\theta\rangle$ is the average cosine of the scattering angle. It should be noted that w may vary with wavelength.

If a medium is illuminated and observed in linearly polarized light whose electric vector is parallel to the scattering plane, the resulting CBOE peak is wider than if the electric vector is perpendicular to the scattering plane (Van Albada *et al.* 1987). Thus, if the incident irradiance is unpolarized, CBOE will be accompanied by a narrow branch of negative polarization (Shkuratov 1989; Muinonen 1990; Mishchenko 1993), which is sometimes referred to as the ''polarization opposition effect.'' Detailed discussions of the phenomenon are given in Hapke (1993) and Shkuratov *et al.* (1994). It was studied in detail by Geake and Geake (1990) and was used to analyze the polarization of light from Saturn's rings by Mishchenko (1993).

The differing dependence of the two mechanisms that cause an opposition effect on such quantities as single and multiple scattering, albedo, polarization, and wavelength suggests a number of different types of tests that might be carried out on the light scattered by a medium in order to elucidate the relative roles of CBOE and SHOE. First, any change that increases the relative contribution of multiple scattering will decrease the amplitude of a SHOE but increase the amplitude of a CBOE, relative to the continuum intensity. Second, if the reflectance is measured in circularly polarized light, a SHOE should be much more pronounced in the helicity-reversing configuration, while a CBOE should be larger in the helicity-preserving configuration. Third the angular width of a CBOE peak depends on wavelength, but that of a SHOE peak does not. Fourth, a polarization opposition effect should accompany a CBOE.

RESULTS

The results of measurements made on two of the lunar samples are given in Figs. 1–4, which show the polarized reflectances of two lunar soil samples, NASA numbers 10084 and 61221, plotted against phase angle. Each reflectance is labeled with a three-letter symbol, whose meanings are as follows. The first letter indicates the orientation of the source polarizer transmission axis relative to the scattering plane (the plane containing the incident and

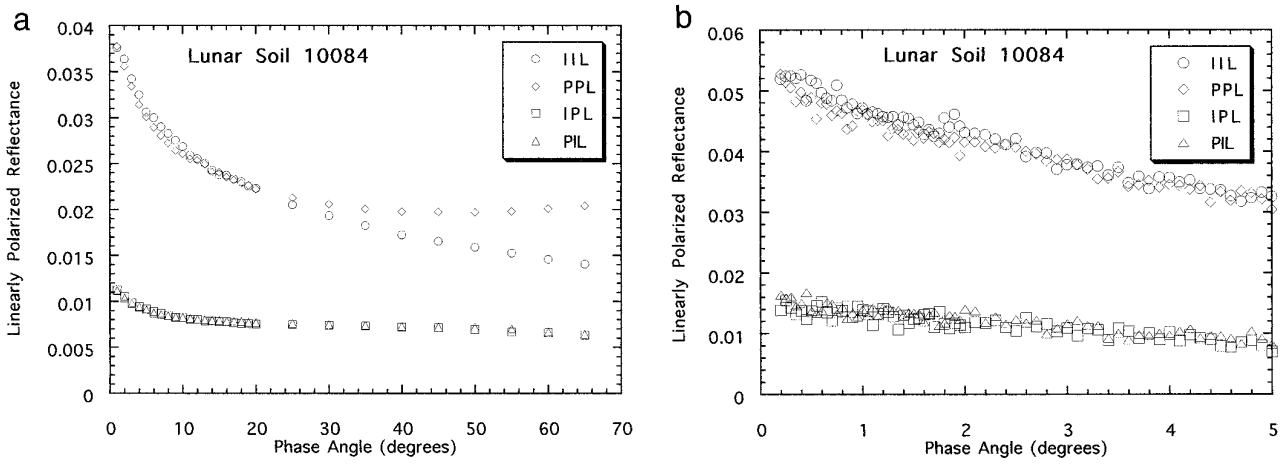

FIG. 1. Linearly polarized reflectances of soil 10084 in red light versus phase angle. Figure 1a gives the short arm data and 1b the long arm data.

scattered rays), with P = perpendicular to and I = in (parallel to) the scattering plane. The second letter similarly indicates the orientation of the detector polarizer axis. The third letter is L or C, where L indicates that the polarizations of the incident and detected intensities were linear, while C indicates that the polarizations were circular. The IIC and PPC reflectances were identical within the measurement errors, so they were averaged to reduce clutter; similarly for the IPC and PIC reflectances. All reflectances were divided by cos$e$ to convert them to values that would have been measured if the detector field of view had been completely filled with illuminated sample surface instead of only partially filled. Finally, the reflectances of each sample were normalized so that their sum equalled the normal albedo of the sample, defined as the reflectance measured at $g = 5°$, relative to a polytetrafluorethylene (halon) pressed powder standard.

Figures 1 and 2 show the linearly polarized reflectances of 10084 and 61221, respectively, at $\lambda = 633$ nm, taken with the short and long arm instruments, plotted against phase angle. Sample 10084 is a dark, high-Ti mare soil with a normal albedo A = 7.8%, and 61221 is an anorthositic highlands soil with an unusually high albedo A = 37.5%. Figures 3 and 4 show the circularly polarized reflectances of these samples. For brevity, the detailed results of measurements on the other samples and at the blue wavelength are not shown, but are qualitatively similar; some were given in a previous paper (Hapke *et al.* 1993).

Errors are about the size of the symbols for the short arm data but are about twice as large as the symbols for

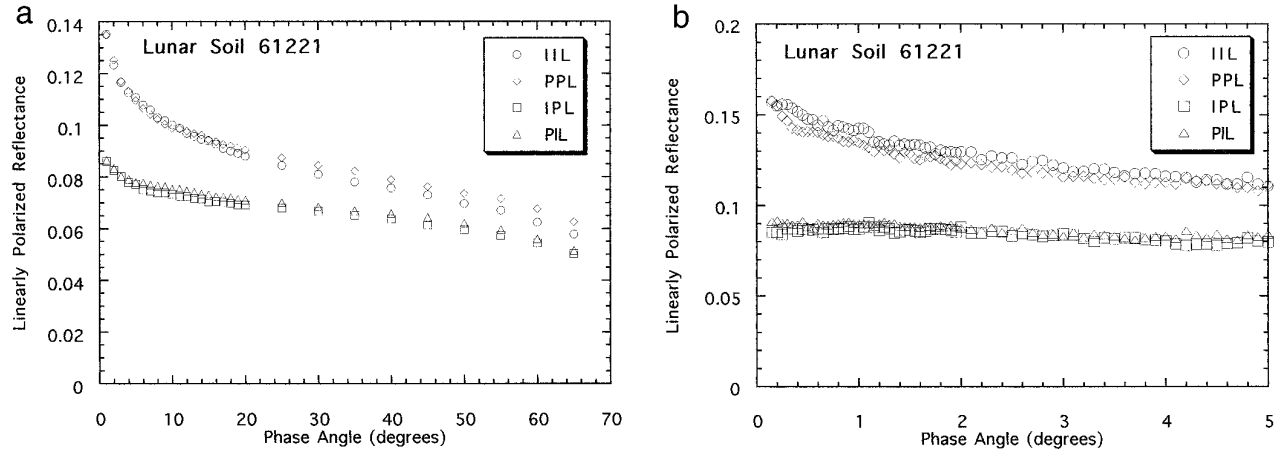

FIG. 2. Linearly polarized reflectances of soil 61221 in red light versus phase angle. Figure 2a gives the short arm data and 2b the long arm data.

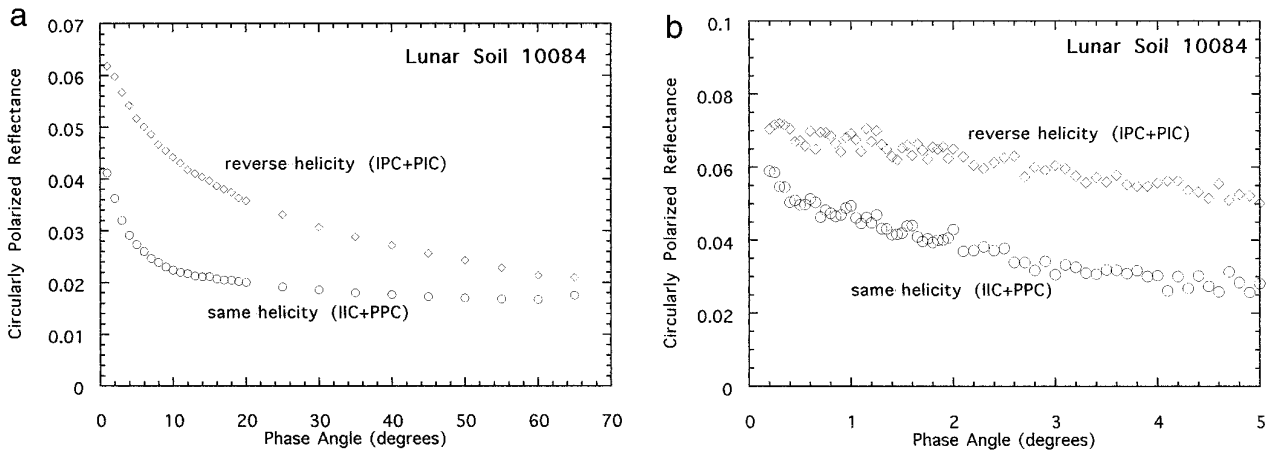

FIG. 3. Circularly polarized reflectances of soil 10084 in red light versus phase angle. Figure 3a gives the short arm data and 3b the long arm data.

the long arm data. As noted previously, most of the noise is caused by laser drift. It will be noted that the reflectances measured with the long-arm photometer are systematically higher than with the short arm one because of the differing angular resolution of the two instruments combined with the highly nonlinear behavior of the opposition peak.

At large phase angles in Figs. 1a and 2a, the IIL and PPL reflectances increase relatively slowly and roughly linearly with decreasing angle down to $g \sim 25°$. PPL exceeds IIL because most of the intensity is produced by specular Fresnel reflection from the surfaces of the soil particles, and is positively polarized. The difference between PPL and IIL is less for 61221 than for 10084 because of the greater contribution of light that has been refracted into the grains of 61221 and internally scattered there, and which is negatively polarized or unpolarized.

Starting at $g \sim 25°$ IIL and PPL both shoot up nonlinearly with decreasing phase angle in a strong opposition effect. A peak this wide has never been reported in the CBOE literature and is difficult to explain by coherent backscattering, but is predicted by shadow hiding. Hence, the width of the peak alone suggests that SHOE is a major contributor to the opposition effect. However, these reflectances contain contributions from both singly and multiply scattered light, so that CBOE could also contribute. PPL is slightly less than IIL over part of this region; when the incident irradiance is unpolarized, this manifests itself as the classical, wide branch of negative polarization discovered by Lyot (1929).

The IPL and PIL reflectances consist mainly of multiply scattered light. They contribute more to the total reflectance of 61221 than that of 10084 because of the higher

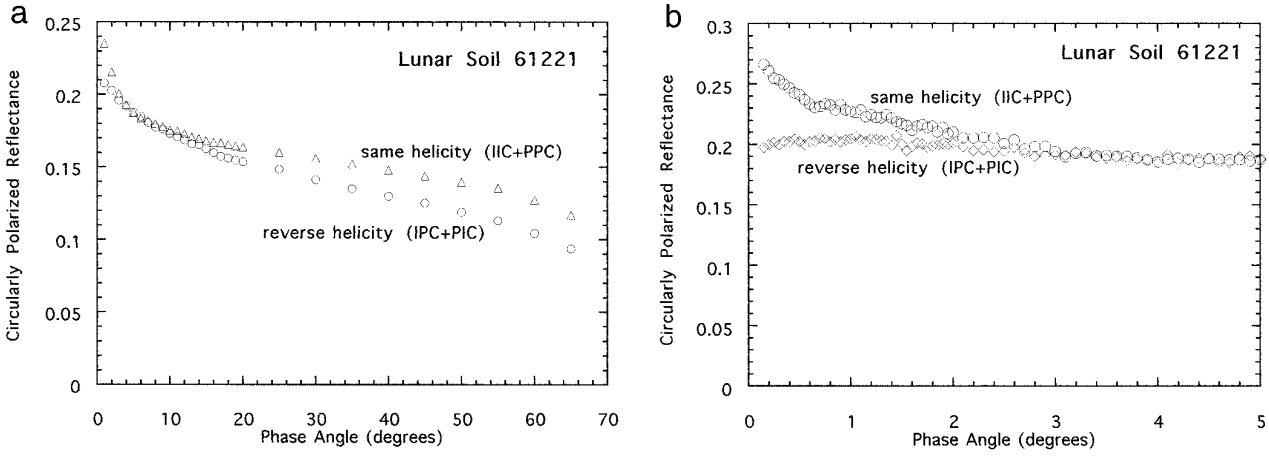

FIG. 4. Circularly polarized reflectances of soil 61221 in red light versus phase angle. Figure 4a gives the short arm data and 4b the long arm data.

albedo of the former. For each sample IPL and PIL are virtually identical, implying that the polarization vectors have been largely randomized. They exhibit a weak opposition effect that is less than 10° wide. Since SHOE is associated almost exclusively with singly scattered light, this opposition effect is surely caused by coherent backscatter.

Figures 1b and 2b show the reflectances taken with the long arm instrument at phase angles less than 5°, well within the opposition effect. Although the PPL and IIL data are nearly the same within experimental errors, the PPL points lie systematically below the IIL for phase angles less than about 3°. This difference appears to be the result of the polarization opposition effect which is specifically predicted to accompany coherent backscattering (Van Albada *et al.* 1987). Consistent with a phenomenon due to multiple scattering, the differences are larger for 61221 than 10084, so that they appear to be real. Such differences would not be expected if the peak were caused exclusively by shadow hiding.

Figures 3 and 4 show the circularly polarized reflectances of the two lunar samples. Both the reverse and same-helicity curves of Figs. 3a and 4a have strong opposition effect peaks. At large phase angles in Fig. 3a the reverse-helicity curve of the low albedo sample 10084 consists almost entirely of light reflected once from the surfaces of the grains, while the same-helicity curve consists of a combination of light transmitted one or more times through particles plus light reflected twice from the grain surfaces. With decreasing phase angle the reverse-helicity reflectances increase relatively slowly down to $g \sim 25°$ and then suddenly surge upward, while the upturn occurs at $g \sim 10°$ for the same-helicity reflectances. The curves in Figure 4a are qualitatively similar, except that the same-helicity curve is larger than the reverse-helicity one because of the increased multiple scattering.

At small phase angles the reverse-helicity curve of the low albedo sample 10084 consists almost entirely of light scattered once from the surface of a grain, either externally or internally, while multiply scattered light makes up most of the contribution to the same-helicity curve. Hence, the broad opposition effect observed in the reverse-helicity curve must be mainly a SHOE, and the narrower surge observed in the same-helicity curve is primarily CBOE. The large peaks in the reverse-helicity curves are very different from those reported in most of the CBOE papers in the literature, which have little or no opposition effect.

The circular polarization ratio μ_c is defined as the ratio of the same-helicity intensity to the reverse-helicity intensity. The sharp, narrow CBOE peak divided by the broad SHOE peak causes μ_c to turn up as the phase angle decreases and enters the CBOE. This behavior is seen in Fig. 5 for all the samples in our possession. It was the criterion used by Hapke *et al.* (1993) to show that coherent backscattering makes an important contribution to the lunar opposition effect.

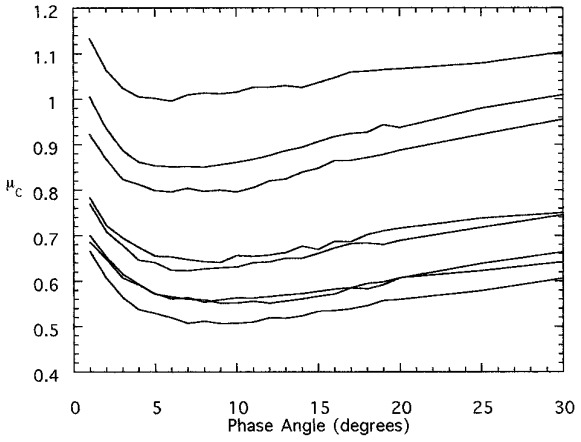

FIG. 5. Circular polarization ratio of all eight soil samples plotted against phase angle.

Unfortunately, no adequate theory presently exists for describing the angular dependence of the opposition effect in a medium of large, irregular particles with a wide size distribution when polarized light is incident and detected. Hence, in order to obtain a rough estimate of the angular width of the peaks, it was assumed that the amplitude of each caused the intensity of the circularly polarized reflectances to double at zero phase. A second order polynomial was fitted to the circularly polarized long arm data, from which the reflectance at zero phase and the phase angle at which the reflectance equals $\frac{3}{4}$ of its zero phase value was determined. This angle was taken as an estimate of the HWHM of the peak. The results are given in Table 1. The HWHM's of the same-helicity peaks, assumed to be primarily CBOE, range from 1.4° to 3.6°, with an average of 2.2°, while the HWHM's of the reverse-helicity peaks, assumed to be primarily SHOE, range from 4.1 to 14.4°, with an average of 8.1°.

According to theory (Etemad *et al.* 1987), a CBOE peak should be sharp only if there is negligible absorption, but should be rounded off in low albedo materials such as lunar regolith. However, the same-helicity curves (Fig. 3b and 4b) are concave upward everywhere and continue to increase nonlinearly, with no sign of rounding down to our instrumental limit of $g = 0.2°$. From Eq. (1), this increase implies that photon paths ~ 10 μm long are contributing to the CBOE at small phase angles.

Thus far, we have discussed only the evidence from the polarized reflectances. However, these quantities require that the incident light be polarized, and so cannot be measured under normal remote sensing conditions where the irradiance is sunlight. We now present some of the data in terms of total reflectance, in which all of the reflectances

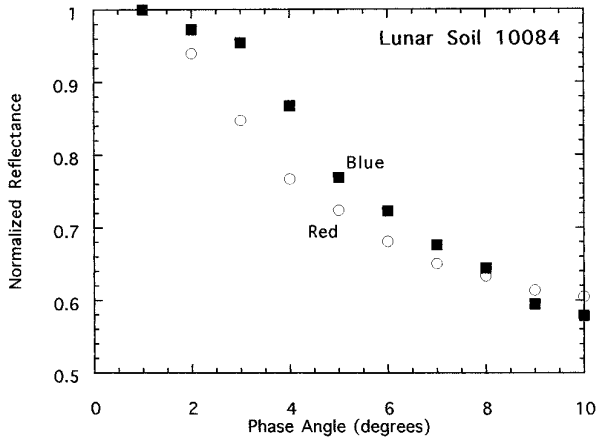

FIG. 6. Total reflectances of soil 10084 measured in red and blue light versus phase angle. The reflectances have been normalized at 1°.

at a given angle are summed and renormalized to their normal albedos relative to halon at 5°. This reflectance is equivalent to what would be observed with unpolarized irradiances and detectors.

Figure 6 shows the reflectance of 10084 measured in red and blue light normalized at $g = 1°$ plotted against g. The albedo of lunar soil increases with wavelength. Hence, from Eqs. (1) and (2), if the opposition effect of lunar regolith were pure CBOE, its angular width should increase faster than linearly with wavelength and should be considerably wider in red than in blue. However, Fig. 6 shows that there is little difference in the angular width; if anything, the peak is slightly wider in blue than in red. This suggests that SHOE dominates the opposition surge.

Figure 7 shows the amplitude of the opposition effect,

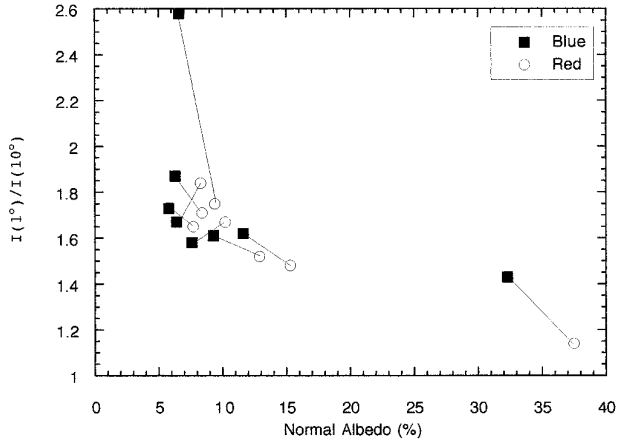

FIG. 7. Amplitude of the opposition effect of all eight samples measured in red and blue light plotted against normal albedo. The lines connect red and blue points for the same sample.

defined here to be the ratio of the intensity at $g = 1°$ to that at 10°, plotted against normal albedo for red and blue light. Since lunar soil is reddish, increasing the wavelength also increases the albedo. Thus, if the opposition effect were pure CBOE, a positive correlation with albedo would be expected, while a negative one would be expected for pure SHOE. Figure 7 shows that the correlation is negative. As the albedo increases, due either to a change in wavelength for the same sample, or to a change in sample composition for different samples, the amplitude decreases in most cases. This again suggests that shadow hiding dominates the opposition effect, at least over this range of phase angles.

Figure 8 plots the ratio of the total reflectances of the lunar samples measured in red light to that in blue light, normalized at $g = 10°$, plotted against phase angle. For SHOE, the opposition peak width is expected to be independent of wavelength and albedo, while the amplitude is independent of wavelength, but decreases with increasing albedo, so that the red/blue ratio should decrease as the phase angle decreases in the peak. For CBOE, the peak amplitude and width both increase with increasing albedo, so that the red/blue ratio should increase as the phase angle decreases. Figure 8 shows that as the phase angle decreases the color ratio decreases down to $g \sim 3°$–$4°$ and then increases. Akimov *et al.* (1979) have previously noted a similar behavior for soil samples returned by Luna spacecrafts. These results suggest that SHOE dominates the opposition effect for $g > 3°$, but that CBOE becomes important for $g < 3°$.

Another relevent observation (not illustrated here) is the fact that the full moon seen in the opposition effect peak does not exhibit either limb darkening or brightening (Wildey 1978). The relative contribution of multiple scattering to the total intensity depends on the angles of incidence and viewing, and decreases as the limb or terminator is approached. Hence, if CBOE were the only process contributing to the lunar opposition effect the full moon would be expected to exhibit pronounced limb darkening, while pure SHOE would cause limb brightening. Although the macroscopic roughness of the lunar surface reduces the size of this effect (Y. Shkuratov, private communication), it should still occur. However, none is observed, probably because SHOE and CBOE have roughly equal amplitudes.

CONCLUSIONS

Several different types of observations lead to the conclusion that neither coherent backscattering nor shadow hiding alone can account for the photometric function of the moon at small phase angles. The reflectances of lunar samples in linearly and circularly polarized light show that the lunar opposition effect appears to be the result of a

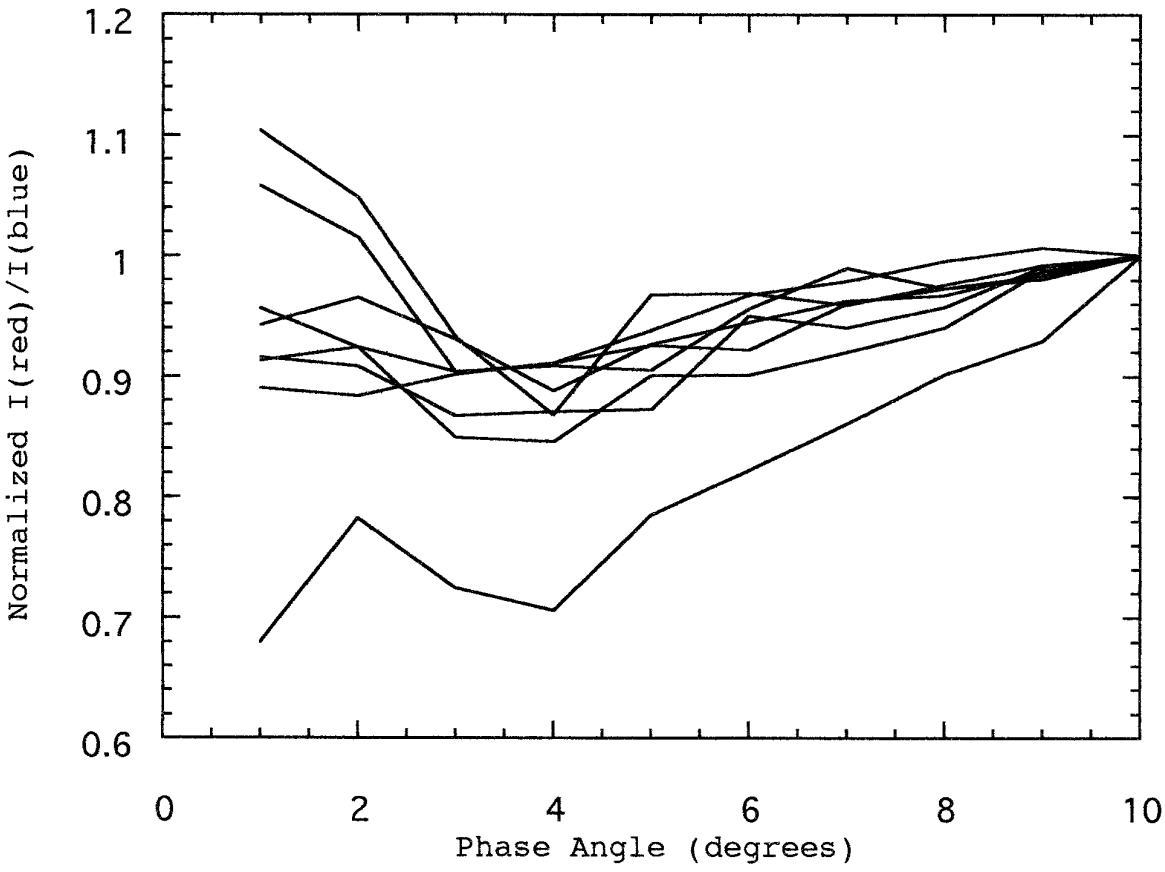

FIG. 8. Ratios of reflectances in red light to that in blue light versus phase angle for all eight samples. The ratios have been normalized at 10°.

narrow CBOE peak with a half-width of about 2° superimposed on a much broader SHOE peak about 8° wide. Helfenstein *et al.* (1997) have arrived at similar values from analysis of a different lunar data set.

The circularly polarized reflectances exhibit SHOE and CBOE peaks that are similar in amplitude, although the SHOE appears to be somewhat larger. The large size and lack of round-off in the CBOE peaks are surprising in a low albedo material such as lunar regolith.

The estimated width of the same-helicity peak of about 2° is interpreted to characterize the CBOE. Hence, Eq. (1) can be used to estimate the transport mean free path L of photons in the medium. This quantity is the average distance a photon propagates before its direction is randomized, and is defined by equation (2). Inserting this value into Eq. (1) gives $L \sim 1$ μm. This value is surprisingly small for media whose mean grain size is of the order of 50 μm (McKay *et al.* 1974). Hence, the CBOE appears to characterize wavelength-sized structures in the regolith, such as fine grains clinging to large ones, rather than the mean particle size.

Mishchenko (1994) and Mishchenko and Macke (1997) have argued that planetary regolith particles, including those of the lunar regolith, are strongly forward scattering because the particle phase functions are dominated by diffracted light, which causes $\langle \cos \theta \rangle$ to nearly equal 1 in Eq. (2). However, if this were the case, L would be expected to be longer than the mean particle size, and certainly much larger than 1 μm. Hence, this value for L does not support Mishchenko's suggestion. (See also Hapke 1996.)

The reverse-helicity peaks, which are interpreted to be primarily SHOE, extend out to phase angles of approximately 25°. It is of interest to note that this is about the same as the width of the classical negative branch of polarization (Lyot 1929), which has never been satisfactorily explained. (See Hapke (1993) and Shkuratov *et al.* (1994) for recent reviews.) This similarity of angular widths strongly suggests that the mechanism that causes this negative polarization is associated with shadow hiding, as postulated by some empirical models, such as that of Wolff (1976).

Lunar soil is an impact-generated regolith, as are most of the surfaces in the solar system, including those on such diverse bodies as Mercury, the asteroids, and the majority of the outer planet satellites. Hence, it is highly likely that

the opposition effects exhibited by these surfaces are dual mixtures of SHOE and CBOE.

No adequate model of the opposition effect which combines shadow hiding and coherent backscattering and accounts for polarization presently exists. A full understanding of the opposition effects and the negative polarizations of solar system bodies will require the construction of theoretical models and the verification of such models by high quality data from lunar samples. We have upgraded our instruments and are currently making improved measurements of lunar and other materials at small phase angles necessary to accomplish this.

ACKNOWLEDGMENTS

We thank A. Verbiscer Skrutskie and especially Y. Shkuratov for constructive reviews that markedly improved this paper. This work was supported by grants from the Planetary Geology and Geophysics Program, Office of Space Science and Applications, National Aeronautics and Space Administration. We also thank Linda Spilker, Tagui Arakelian, Vacik Gharakanian, and Paul Herrera for their assistance.

REFERENCES

Akimov, L., I. Antipova-Karataeva, and Y. Shkuratov 1979. Indicatrix measurements of lunar samples from landing sites of Luna 24, Luna 16 and Luna 20. *Lunar and Planetary Science*, vol. X, pp. 9–11.

Buratti, B., J. Hillier, and M. Wang 1996. The lunar opposition surge: Observations by Clementine. *Icarus* **124,** 490–499.

Etemad, S., R. Thompson, M. Andrejco, S. John, and F. MacKintosh 1987. Weak localization of photons: Termination of coherent random walks by absorption and confined geometry. *Phys. Rev. Lett.* **59,** 1420–1423.

Geake, J., and M. Geake 1990. A remote-sensing method for sub-wavelength grains on planetary surfaces by optical polarimetry. *Mon. Not. Astr. Soc.* **245,** 46–55.

Gehrels, T., Coffeen, D., and Owings, D. 1964. Wavelength dependence of polarization. III. The lunar surface. *Astron. J.* **69,** 826–852.

Hapke, B. 1986. Bidirectional reflectance spectroscopy. 4. Extinction and the opposition effect. *Icarus* **67,** 246–280.

Hapke, B. 1990. Coherent backscatter and the radar characteristics of outer planet satellites. *Icarus* **88,** 407–417.

Hapke, B. 1993. *Theory of Reflectance and Emittance Spectroscopy.* Cambridge Univ. Press, New York.

Hapke, B. 1996. Are planetary regolith particles back scattering? Response to a paper by M. Mishchenko. *J. Quant. Spectrosc. Radiat. Transfer* **55,** 837–848.

Hapke, B., D. DiMucci, R. Nelson, and W. Smythe 1996. The cause of the hot spot in vegetation canopies and soils: Shadow-hiding versus coherent backscatter. *Remote Sens. Environ.* **58,** 63–68.

Hapke, B., R. Nelson, and W. Smythe 1993. The opposition effect of the moon: The contribution of coherent backscatter. *Science* **260,** 509–511.

Helfenstein, P., J. Veverka, and J. Hillier 1997. The lunar opposition effect: A test of alternative models. *Icarus* **128,** 2–14.

Kaveh, M., M. Rosenbluh, I. Edrei, and I. Freund 1986. Weak localization and light scattering from disordered solids. *Phys. Rev. Lett.* **57,** 2049–2052.

Kravtsov, Y., and A. Saichev 1982. Effects of double passage of waves in randomly inhomogeneous media. *Sov. Phys. Uspekhi.* **25,** 494–508.

Kuga, Y., and A. Ishimaru 1984. Retroreflectance from a dense distribution of spherical particles. *J. Opt. Soc. Am. A* **1,** 831–835.

Lyot, B. 1929. Recherches sur la polarisation de la lumiere des planetes et de quelques substances terrestres. *Ann. Obs. Paris,* Vol. VIII, Book 1. [Translated as NASA Tech. Transl. TT-F-187, 1964]

McKay, D., R. Furland and G. Heiken (1974). Grain size and the evolution of lunar soils. In *Proc. 5th Lunar Sci. Conf.* (W. Gose, Ed.), pp. 887–906. Pergamon, New York.

Mishchenko, M. 1993. On the nature of the polarization opposition effect exhibited by Saturn's rings. *Astrophys. J.* **411,** 351–361.

Mishchenko, M. 1994. Asymmetry parameters of the phase function for densely packed scattering grains. *J. Quant. Spectrosc. Radiat. Transfer* **52,** 95–110.

Mishchenko, M., and J. Dlugaach 1992. Can weak localization of photons explain the opposition effect of Saturn's rings?. *Mon. Not. Roy. Astron. Soc.* **254,** 15–18.

Mishchenko, M., and A. Macke 1997. Asymmetry parameters of the phase function for isolated and densely packed particles with multiple internal inclusions in the geometric optics limit. *J. Quant. Spectrosc. Radiat. Transfer*, **57,** 767–794.

Muinonen, K. 1990. *Light Scattering by Inhomogeneous Media: Backward Enhancement and Reversal of Linear Polarization.* Ph.D. dissertation, University of Helsinki, Finland.

Seeliger, H. 1895. Theorie der Beleuchtung staubformiger kosmischen Masses insbesondere des Saturinges. *Abh. Bayer. Acad. Wiss. Math.-Naturwiss. Kl.* **18,** 1–72.

Shkuratov, Y. 1988. Diffractional model of the brightness surge of complex structure surfaces. *Kin. Phys. Cel. Bodies* **4,** 33–39.

Shkuratov, Y. 1989. New mechanism of formation of negative polarization of light scattered by the solid surfaces of cosmic bodies. *Solar System Res.* **23,** 111–113.

Shkuratov, Y., K. Muinonen, E. Bowell, K. Lumme, J. Peltoniemi, M. Kreslavsky, D. Stankevich, V. Tishkovetz, N. Opanasenko, and L. Melkumova 1994. A critical review of theoretical models of negatively polarized light scattered by atmosphereless Solar System bodies. *Earth Moon Planets* **65,** 201–246.

Van Albada, M., and A. Lagendijk 1985. Observation of weak localization of light in a random medium. *Phys. Rev. Lett.* **55,** 2692–2695.

Van Albada, M., M. Van der Mark, and A. Lagendijk 1987. Observation of weak localization of light in a finite slab: Anisotropy effects and light-path classification. *Phys. Rev. Lett.* **58,** 361–364.

Van Albada, M., M. Van der Mark, and A. Lagendijk 1990. Experiments on weak localization of light and their interpretation. In *Scattering and Localization of Classical Waves in Random Media* (P. Sheng, Ed.), pp. 97–136. World Scientific, Teaneck.

Wildey, R. 1978. The moon in heiligenschein. *Science* **200,** 1265–1267.

Watson, K. 1969. Multiple scattering of electromagnetic waves in an underdense plasma. *J. Math. Phys.* **10,** 688–702.

Wolff, M. 1975. Polarization of light reflected from rough planetary surface. *Appl. Opt.* **14,** 1395–1405.